Science Advances
AAAS

advances.sciencemag.org/cgi/content/full/5/4/eaau3112/DC1

Supplementary Materials for

Secondary nucleation and elongation occur at different sites on Alzheimer's amyloid-β aggregates

Tom Scheidt, Urszula Łapińska, Janet R. Kumita, Daniel R. Whiten, David Klenerman, Mark R. Wilson, Samuel I. A. Cohen, Sara Linse, Michele Vendruscolo, Christopher M. Dobson, Tuomas P. J. Knowles*, Paolo Arosio*

*Corresponding author. Email: tpjk2@cam.ac.uk (T.P.J.K.); paolo.arosio@chem.ethz.ch (P.A.)

Published 17 April 2019, *Sci. Adv.* **5**, eaau3112 (2019)
DOI: 10.1126/sciadv.aau3112

This PDF file includes:

Supplementary Material

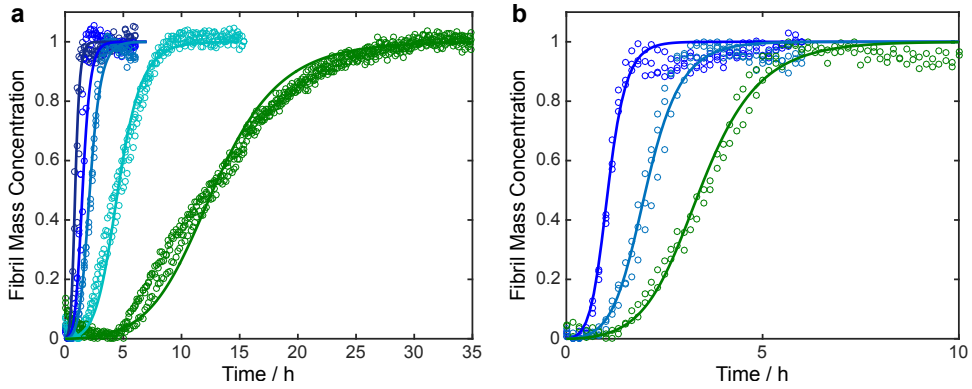

Fig. S1. Analysis of the effects of clusterin on the aggregation kinetics of Aβ(M1-42) at 37°C.(a) Kinetic reaction profiles at 37°C for the aggregation of 3 μM Aβ(M1-42) solutions are shown from left (blue) to right (green) in the absence and presence of 7.5 nM, 37 nM, 75 nM and 150 nM of clusterin. Continuous lines represent integrated rate laws where the elongation rate constant has been specifically inhibited. b) Same as in a) in the absence and presence of 37 nM and 75 nM of clusterin. The average least-squares error function of these simulations, defined in the Materials and Methods section, is 0.1.

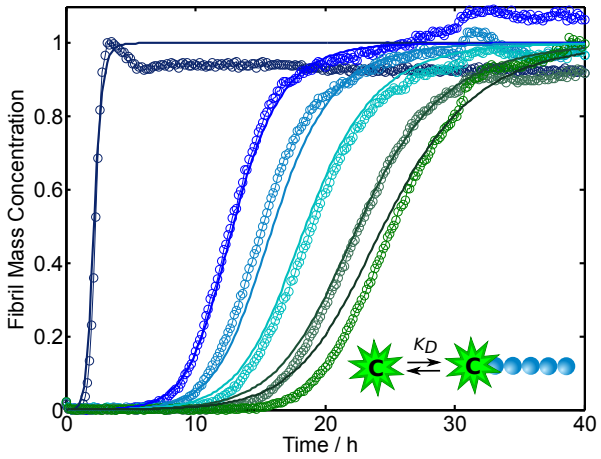

Fig. S2. Analysis of the effects of clusterin on the aggregation kinetics of Aβ(M1-42) at 21°C. Aβ(M1-42) aggregation kinetics are shown from left (blue) to right (green) in the absence and presence of 40 nM, 60 nM, 80 nM, 120 nM and 140 nM of clusterin (symbols) with an Aβ(M1-42) monomer concentration of 4 μM. The data was globally fitted similar to the procedure at 37°C in fig. S2 (continuous lines) in order to determine the dissociation constant $\mathrm{K_{D,21^{\circ}C}} = 1$ nM at this temperature.

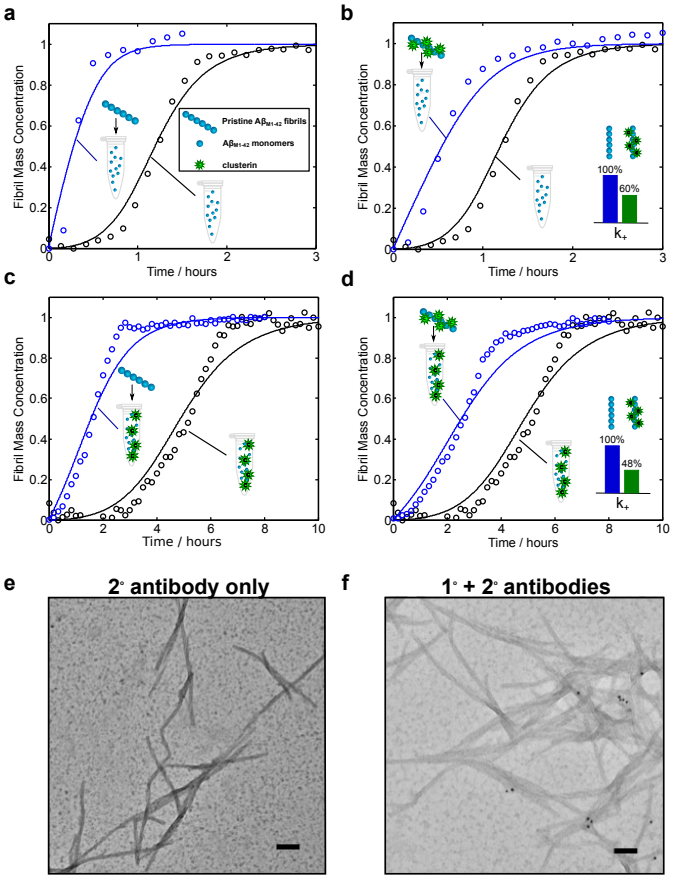

Fig. S3. Seeding experiments of Aβ(M1-42) in the presence and absence of clusterin. Aggregation profiles of reactions where pre-formed Aβ(M1-42) fibrils, grown in the presence or absence of clusterin, were added to monomeric solutions of Aβ(M1-42) in the presence or absence of the chaperone. (a) Pristine fibrils that had never been exposed to the chaperone (blue $\circ$) were able to accelerate the aggregation reaction of Aβ(M1-42) monomers compared to the kinetics in the absence of added pre-formed fibrils (black symbols). (b) Fibrils grown in the presence of 37 nM clusterin (blue $\circ$) did not accelerate the reaction to the same extent as pristine fibrils when added to monomer without the chaperone in solution (black $\circ$), showing that clusterin binds to fibrils. (c, d) Clusterin added in solution is able to arrest the reaction and prevent the acceleration due to added fibrils (blue $\circ$) even when the latter were grown in the absence of chaperone. The solution concentrations of Aβ(M1-42) and clusterin were 2 μM and 37 nM, respectively. The amount of added seeds has been 5% w/w for all seeded experiments. The dashed lines show predictions for the reaction profiles of seeded and unseeded reactions assuming (a) the value of the elongation rate constant measured previously in the absence of the chaperone, *(10)* (b) the value in (a) reduced to 60% of its value, and (c,d) the elongation rate reduced to 48% with additional chaperones in the Aβ(M1-42) monomer solution. (e,f) Aβ(M1-42) fibrils formed in the presence of BSA and clusterin and probed for clusterin interaction using immunogold TEM. (e) sample probed with only the secondary antibody conjugated to a gold particle showing no non-specific labelling; (f) fibrils probed with an anti-clusterin monoclonal antibody followed by an anti-mouse secondary antibody conjugated to a gold particle. Black dots indicate the presence of clusterin interacting with the fibrils. Scale bar is 100 nm.

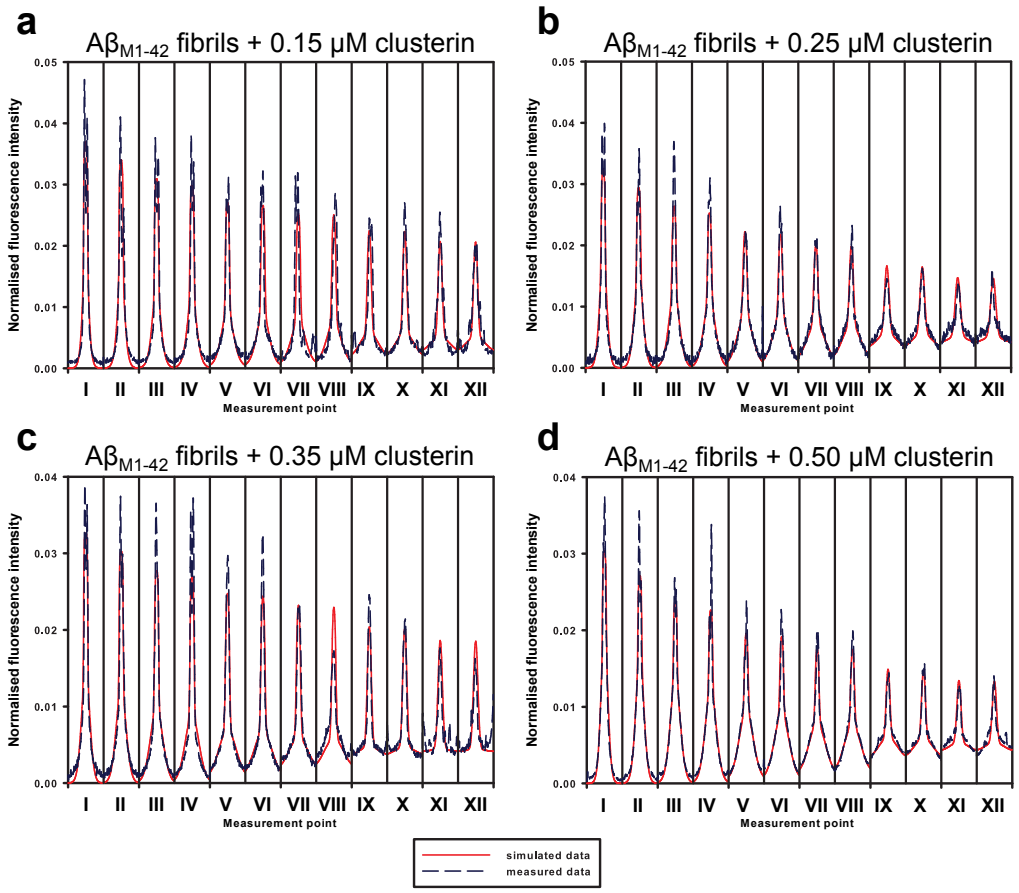

Fig. S4. Diffusion profiles of specific samples at 12 different positions in a microfluidic device.(a-d) Representative fluorescence diffusion profiles corresponding to solutions of 17 μM Aβ(M1-42) fibrils in the presence of different clusterin concentrations acquired at twelve different positions along the channel. The simulated diffusion profiles (red lines) were fitted to the measured data (black dashed lines) by a least square fit.

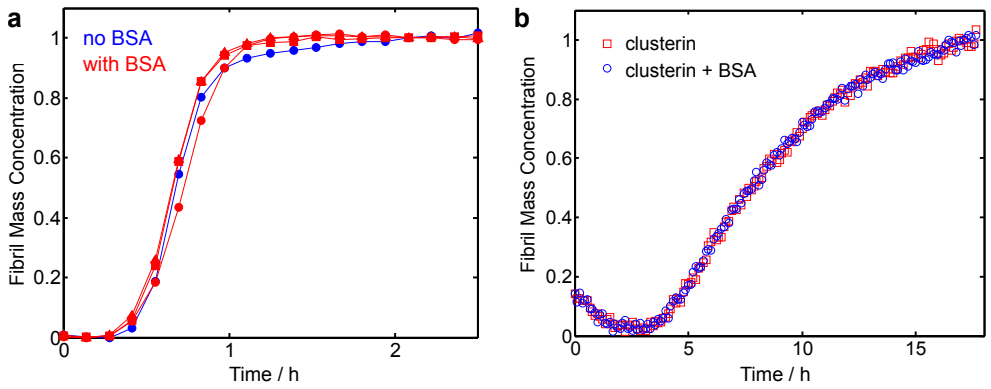

Fig. S5. Analysis of interfering effects of transient proteins on clusterin inhibition activity. (a) Kinetic reaction profiles for the aggregation of 2 μM Aβ(M1-42) in the absence (blue symbols) and presence (red symbols) of 7.5 nM, 37 nM and 75 nM of bovine serum albumin (BSA). (b) Same as in a) but in the presence of 75 nM of BSA and 75 nM of clusterin, showing that the presence of BSA does not affect the inhibition activity of clusterin.

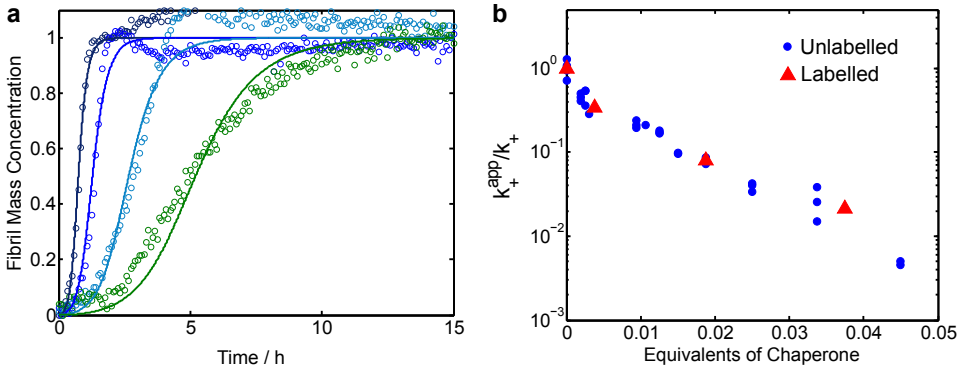

Fig. S6. Effects of the fluorescent label of clusterin on the inhibition process on Aβ(M1-42) aggregation.(a) Kinetic reaction profiles for the aggregation of 2 μM Aβ(M1-42) solutions are shown from left (blue) to right (green) in the absence and presence of 7.5 nM, 37 nM and 75 nM of labelled clusterin. Continuous lines represent model simulations where the elongation rate constant has been specifically inhibited; (b) The decrease in the apparent elongation rate constant as a function of molecular chaperone concentration is similar for labelled and unlabelled clusterin.

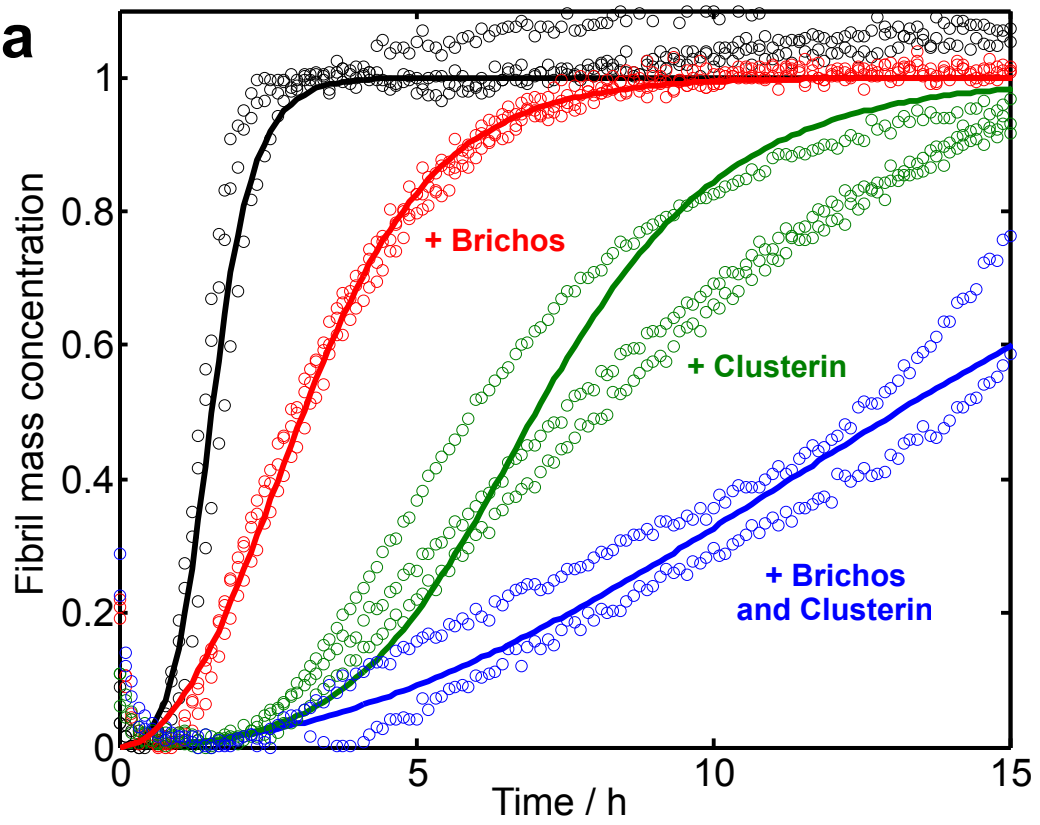

Fig. S7. Kinetic analysis on the aggregation kinetics of Aβ(M1-42) in the presence of Brichos and clusterin separately and combined. Kinetic reaction profiles for the aggregation of 2.5 μM Aβ(M1-42) solutions in 20 mM sodium phosphate buffer at pH 8.0 in the absence and presence of 37 nM clusterin and 3 μM proSP-C Brichos, added either individually or together as indicated at 37°C. Continuous lines represent model simulations where either the elongation rate constant (green line), secondary nucleation constant (red line) or both (blue line) have been selectively inhibited.